JAAS

ROYAL SOCIETY OF CHEMISTRY

PAPER

View Article Online
View Journal | View Issue

Cite this: *J. Anal. At. Spectrom.*, 2025, 40, 1343

Cutting-edge arsenic quantification in pyrolysis oils: evaluation of a high temperature torch integrated sample introduction system (hTISIS) combined with an ICP-MS/MS†

Mar Todolí-Carbonell, [a] Rebeca Pérez-Ramírez, [a] Thomas Coquet,[b] Fabien Chainet, [b] Marion Lacoue-Nègre[b] and Raquel Sánchez-Romero *[a]

An innovative approach for routine arsenic quantification in complex tire pyrolysis oil (TPO) matrices by combining a high temperature torch integrated sample introduction system (hTISIS) with ICP-MS/MS is presented. Tire pyrolysis oils present significant potential as alternative fuels but require precise monitoring of arsenic due to its environmental toxicity and its detrimental effects on catalytic processes. The hTISIS system, operating at 400 °C, significantly enhanced analyte transport efficiency, increasing the signal by up to 20-fold compared to conventional sample introduction systems. Moreover, the method achieved detection limits as low as 2 ng kg^{-1} for arsenic in xylene, significantly lower than the 20 ng kg^{-1} obtained using conventional sample introduction systems. Moreover, procedural limit of quantification (pLOQ) obtained for the hTISIS system was 60 ng kg^{-1}. Additionally, the combination of hTISIS working at 400 °C and ICP-MS/MS successfully mitigated matrix effects and spectral interferences by employing oxygen as a reaction gas, allowing accurate quantification even in samples containing high chlorine levels. Analysis of 13 TPO samples showed arsenic concentrations ranging from 41 ± 4 to 924 ± 80 μg kg^{-1}. The results were validated through comparison with microwave digestion method, showing no statistically significant differences for most samples with a confidence level of 95%.

Received 3rd March 2025
Accepted 3rd April 2025

DOI: 10.1039/d5ja00081e

rsc.li/jaas

1. Introduction

Pyrolysis of end-of-life tires enables the recovery of valuable resources like tire pyrolysis oil (TPO), carbon black, steel, and syngas, thereby promoting a circular economy.[1] These materials could be reused in industries, reducing waste and environmental impact while enhancing energy efficiency.[2] Specifically, TPO is a promising fraction due to its high calorific value, comparable to that of heavy fuel oil, making it a viable alternative fuel or a valuable feedstock for refineries. With up to 65% biogenic carbon content, TPO refining presents significant potential for integration into bio-based fuel production pathways.

TPO is a complex mixture of aliphatic, aromatic, heteroatomic, and polar compounds, with boiling points ranging from 70 to 550 °C, depending on process conditions and feedstock properties. As reported in the literature,[1,3,4] the main physicochemical properties of TPO are very similar to those of conventional refinery fractions, facilitating its processing or co-processing with fossil feedstocks without requiring major modifications to existing refining units. However, certain properties, such as the content of heteroatomic compounds (N, S, O) and aromatics with widely varying boiling points[1,5] as well as the presence of metals and metalloids (*e.g.*, As, Br, Cl, Cd, Cr, Fe, Si, Pb, Zn),[4,6–8] can fluctuate significantly depending on the production process. In this case, a complete upgrading of the TPO (mainly as hydroprocessing) is required to remove these contaminants, improve the properties of the oil and fulfill the fuel specifications without deactivating the catalysts.[1,3–5,9]

The rigorous monitoring of metals and metalloids in fuels and alternative fuels is essential due to their environmental and operational impact.[10–13] In particular, controlling arsenic levels in TPO is crucial for regulatory compliance and industrial efficiency. Arsenic can generate toxic emissions during combustion, deteriorating air quality and posing health risks.[12] Moreover, it acts as a catalyst poison in refining and gas treatment processes, reducing efficiency and increasing operational costs.[13]

Spectroscopic analytical techniques such as graphite furnace atomic absorption spectrometry (GFAAS),[14] electrothermal atomic absorption spectrometry (ETAAS),[15–19] inductively coupled plasma optical emission spectroscopy (ICP-OES)[19–21]

[a]*Department of Analytical Chemistry, Nutrition and Food Sciences, University of Alicante, 03690, San Vicente del Raspeig, Alicante, Spain. E-mail: r.sanchez@ua.es*
[b]*IFP Energies Nouvelles, Rond-point de l'échangeur de Solaize, BP 3, 69360 Solaize, France*

† Electronic supplementary information (ESI) available. See DOI: https://doi.org/10.1039/d5ja00081e

and mass spectrometry (ICP-MS), have been recommended to carry out the arsenic determination in these organic samples.[11,15,22–32] Among these, ICP-MS is particularly valued for its high sensitivity, low detection limits, and capability to simultaneously detect multiple elements.[33] However, the introduction of organic samples into the plasma could lead to issues such as thermal degradation of the plasma, polyatomic interferences, and soot accumulation on the torch or ICP-MS interface cones, which is often mitigated by adding an oxygen stream.[34] Additionally, the accuracy of arsenic determinations could be compromised by variations in the ICP-MS signals of different species of the same element.[25,35–37]

Significant spectral and non-spectral interferences have been identified that could degrade the accuracy of determinations using ICP-MS. ICP-tandem mass spectrometry (ICP-MS/MS)[38,39] mitigates spectral interferences, which makes it especially suitable for quantifying elements like arsenic, which may face spectral interferences. For example, ions like $^{40}Ar^{35}Cl^{+}$, $^{38}Ar^{37}Cl^{+}$, $^{59}Co^{16}O^{+}$, $^{40}Ca^{35}Cl^{+}$, Sm^{2+} and $^{150}Nd^{2+}$ could overlap with peaks of isotope $^{75}As^{+}$.[40–42] Sample preparation methods, particularly dilution with organic solvents or matrix acid digestion, have been developed to minimize matrix effects, although high dilution factors could increase the limits of quantification.[10,11,13,15,23,25]

The so-called high temperature torch integrated sample introduction system (hTISIS) has been designed to improve the ICP analytical performance by enhancing analyte transport efficiency, which can be nearly 100% under optimized conditions.[43,44] This enhancement leads to improved sensitivity and reduced matrix effects, allowing for the implementation of a universal calibration procedure.[45,46] However, the main challenge associated with this system is the high solvent load reaching the plasma, which may cause issues such as thermal degradation or soot formation. To mitigate this, previous studies explored air-segmented injection procedures, which produce transient signals and limit solvent introduction.[43–45,47,48] While effective in minimizing solvent-related issues, air-segmented injection is less compatible with routine analysis due to its operational complexity.[46] For this reason, continuous sample aspiration is preferred in routine applications, as it offers greater simplicity and suitability for high-throughput workflows. The use of hTISIS under continuous aspiration, combined with the polyatomic interference removal capabilities of ICP-MS/MS, enables accurate analysis of complex organic matrices, including oils, fats, biofuel precursors, and light petroleum products.[46,49]

In this context, the goal of the present study was to combine the advantages of hTISIS and ICP-MS/MS to achieve accurate quantification of arsenic in tire pyrolysis oil (TPO) samples under routine analysis conditions using continuous sample aspiration.

2. Experimental

2.1. Reagents and samples

Arsenic solutions were prepared by dissolving an arsenic monoelemental stock organic standard solution (1000 mg kg^{-1}, Conostan®, SCP SCIENCE, Clark Graha, Baie D'Urfé, Canada). Moreover, arsenic solutions were prepared by using trimethylarsine (TMA), triethylarsine (TEA) from Strem chemical Europe (Bischheim, France), and triphenylarsine (TPA) from Sigma Aldrich (Saint-Quentin-Fallavier, France). Additionally, 5000 mg kg^{-1} chlorine standard solution (Conostan®, SCP SCIENCE, Clark Graha, Baie D'Urfé, Canada) was used for the evaluation of spectral interferences. And 1000 mg kg^{-1} yttrium solution (Conostan®, SCP SCIENCE, Clark Graha, Baie D'Urfé, Canada) was used as internal standard. In order to investigate matrix effects, four different solvents were studied: xylene, kerosene and toluene, purchased from Labbox (Labbox Labware S.L., Vilassar de Dalt, Barcelona, Spain); and PremiSolv® solvent purchased from Conostan® (Conostan®, SCP SCIENCE, Clark Graha, Baie D'Urfé, Canada).[50] Moreover, to evaluate the accuracy of the method, the NIST 1634c trace elements in fuel oil standard reference sample was analyzed (National Institute of Standards and Technology, Gaithersburg, USA).

Thirteen tire pyrolysis oils (TPOs) (IFPEN, Solaize, France), sourced from commercial providers and originating from different types of tires (cars, trucks or others) and various countries have been analyzed. To avoid the heterogeneity of sampling, all the TPO samples were previously filtered at 1.6 μm (Whatman® glass microfiber filters, Grade GF/A) before analysis. The analytical methods used to characterize the TPO were previously described in Badlaoui *et al.*[4] Chlorine and silicon concentrations were determined by wavelength dispersive X-rays fluorescence (Axios from Panalytical, Almelo, Netherlands) following an in-house method. The main physiochemical properties of the TPOs are summarized in Table S1,† highlighting the significant diversity among the selected samples. Their boiling point ranges varied widely (83 < T5 wt% (°C) < 206 and 392 < T95 wt% (°C) < 555), total aromatic content ranged from 38 to 72 wt%, nitrogen between 1450 and 7630 mg kg^{-1} and chlorine concentration from below 5 to up to 865 mg kg^{-1}.

For accuracy and reproducibility studies, some selected samples were spiked at different arsenic concentration levels with an arsenic standard solution (1000 mg kg^{-1}, Conostan®, SCP SCIENCE, Clark Graha, Baie D'Urfé, Canada). To perform the analysis according to the dilution method, liquid oil samples were manually shaken for 1 minute. After that, a given mass of the sample was weighed and properly diluted with xylene. A dilution factor of 10 was applied to the samples.

2.2. Instrumentation

Arsenic content was measured by using an Agilent 8900 ICP-QQQ instrument (Agilent Technologies, CA, USA) in the single quad mode and in the mass-shift mode using oxygen as a reaction gas. This instrument is equipped with an octupole collision-reaction cell (CRC) located in-between two quadrupole analysers, thus allowing to minimize spectral interferences. Different gas modes (no gas and O_2 mode) were employed. Moreover, a mixture of argon/oxygen (80/20) as optional gas was added to mitigate carbon deposits (Table 1).

The sample introduction system was a conikal nebulizer (Glass Expansion, Melbourne, Australia) and a high

Table 1 ICP-MS/MS operating conditions

	hTISIS	Conventional
Spray chamber	Single pass	Scott double-pass
Nebulizer	Conikal	Conikal
RF power (kW)	1.6	1.6
Plasma flow (L min^{-1})	15	15
Auxiliary flow (L min^{-1})	1	1
Nebulizer flow (L min^{-1})	0.4	0.4
Option gas (L min^{-1}) (Ar 80%, O_2 20%)	0.4	0.4
Makeup gas (L min^{-1})	—	0.3
Spray chamber temperature (°C)	400	−5
Sampling depth (mm)	8	8
Liquid flow (μL min^{-1})	30	100
Scan type	MS/MS	MS/MS
Replicates	5	5
Collision/reaction gases	O_2 (0.075 mL min^{-1})	O_2 (0.075 mL min^{-1})
Stabilization time (s)	No gas: 10 O_2: 30	No gas: 10 O_2: 30
Sweeps	10	10
Measured isotopes	No gas: $^{75}As^+$, $^{36}Ar^+$, $^{89}Y^+$ O_2 gas: $^{75\rightarrow75}As^+$, $^{75\rightarrow91}AsO^+$, $^{36}Ar^+$, $^{89}Y^+$	

temperature Torch Integrated Sample Introduction System (hTISIS),[43,44] equipped with a 47 cm^3 single-pass spray chamber. A copper coil was wound around the spray chamber and its temperature was set by means of a temperature controller (Design Instruments, Barcelona, Spain). The solutions were delivered in continuous sample aspiration mode to the nebulizer by means of a peristaltic pump Perimax 16 antiplus, (Spetec GmbH, Erding, Germany) and a 0.25 mm id flared end solva tubing (Glass Expansion, Melbourne, Australia). A conventional Scott double-pass spray chamber cooled at −5 °C coupled to the conikal nebulizer was taken as a reference system. The selected operating conditions are summarized in Table 1.

2.3. Sample digestion

As reference method, microwave-assisted acid digestion followed by ICP-MS analysis was selected. Samples were digested using a microwave digestion system Start D (Milestone, Sorisole, Italy). Approximately 0.5 g (with a precision of ± 0.1 mg) of sample were transferred to a digestion vessel and then 6.0 mL of 65% HNO_3 (Labbox Labware S.L., Vilassar de Dalt, Barcelona, Spain) and 1 mL of 30% H_2O_2 (ScharLab S.L., Sentmenat, Barcelona, Spain) were added. Samples were digested at 200 °C for 30 min. Final digests were transferred to plastic vessels and diluted to 20 g with Milli-Q water (Millipore, El Paso, TX, USA). The digests were finally analyzed through ICP-MS by means of an Agilent 7700 spectrometer (Santa Clara, California) using external calibration and on-line addition of internal standards for quantification. The sample introduction system was a conventional Scott double-pass spray chamber cooled at −5 °C coupled to a pneumatic concentric nebulizer.

3. Results and discussion

Determining trace concentrations of arsenic in complex organic samples presents several challenges, including spectral interferences, the impact of arsenic's chemical form on the signal, and matrix effects. Therefore, it is essential to develop a straightforward routine analysis method that simultaneously addresses and minimizes these issues without compromising any analytical figures of merit.

3.1. As spectral interferences

3.1.1. Effect of the reaction cell gas flow rate. Mitigating spectral interferences is crucial for accurate arsenic determination, particularly in complex matrices like pyrolysis oils, which could contain significant levels of chlorine. Chlorine concentrations in the 13 selected TPOs in this study have been reported to range from a few mg kg^{-1} up to 865 mg kg^{-1} (Table S1†). This high chlorine content could compromise the accuracy of arsenic determination due to spectral interferences. In ICP-MS/MS, using O_2 as a reaction gas, $^{75}As^+$ ions could be converted to the corresponding $^{75}As^{16}O^+$ reaction product ion, effectively mitigating these interferences.[51] The conversion efficiency was initially evaluated. The mass-to-charge ratio (m/z) of the first quadrupole was fixed at 75, while the second

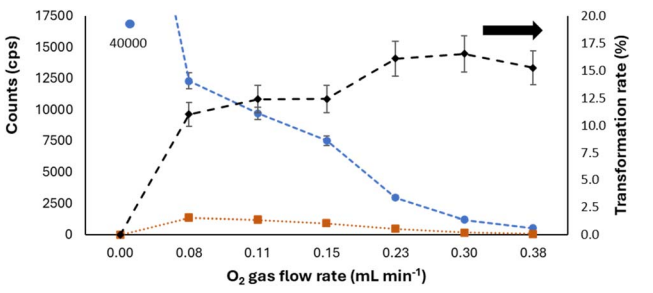

Fig. 1 Effect of the oxygen flow rate on the ionic signal obtained at m/z = 75 (blue circles), m/z = 91 (orange squares), and on the transformation rate (black circles, secondary axis). ICP-MS/MS operating conditions described in Table 1. As concentration: 25 μg kg^{-1} using Conostan based solution.

quadrupole was set at 75 and 91. Fig. 1 shows that at high oxygen reaction gas flow rates, the signal at $m/z = 91$, accounted for approximately 17% of the signal measured at $m/z = 75$, thus indicating low efficiency in the formation of $^{75}As^{16}O^{+}$ ion. Consequently, the analytical response, when considering $m/z =$ 91, was significantly lower than those found for the m/z of the predominant isotope of As ($m/z = 75$). Additionally, an increase in the oxygen gas flow rate led to a significant drop in the signal obtained for $^{75}As^{+}$ (Fig. 1). This phenomenon could be attributed to the defocusing of these ions caused by the addition of O_2 to the collision/reaction cell.[52] When the signal was measured at m/z ratio of 91, an increase in the intensity was observed, reaching a maximum at 0.075 mL min^{-1} of oxygen (Fig. 1). Beyond this oxygen gas flow rate, the signal decreased due to the defocusing effect caused by an excessive increase in the concentration of oxygen molecules in the reaction cell.[52]

For the optimal oxygen gas flow rate, the impact of the presence of chlorine in the sample solution was evaluated. It was verified that, as Fig. S1† shows, using oxygen at a flow rate of 0.075 mL min^{-1} enabled the mitigation of chlorine contribution to the analytical signal obtained in on mass mode up to a concentration of 750 mg Cl per L (Fig. S1†). It was observed that, at 750 mg L^{-1} of chlorine, the signal produced at m/z 75 was 5% of that obtained for a xylene 25 μg kg^{-1} As solution. As expected, for m/z 91 (mass shift mode), chlorine contribution to the As intensity was negligible even at 750 mg kg^{-1} of chlorine. In fact, for this chlorine content, the analytical signal enhancement was lower than 2% (Fig. S2†).

3.2. Use of hTISIS for arsenic determination

Arsenic determination requires a highly sensitive system, as its concentration in samples from pyrolysis oils is typically low. In this context, the hTISIS offers several advantages over the conventional sample introduction system, because it affords 100% analyte transport efficiency regardless of the sample nature, thereby enhancing sensitivities as compared to conventional systems.[43–47] Therefore, hTISIS spray chamber temperature is crucial, as it influences both signal intensity and matrix effects. To evaluate the impact of hTISIS temperature on the signal, an improvement factor (f_{imp}) was calculated by applying the eqn (1):

$$f_{imp} = \frac{I_i^{hTISIS}}{I_i^{Conventional}} \times \frac{Q_l^{Conventional}}{Q_l^{hTISIS}} \quad (1)$$

where I_i was the obtained signal for an m/z ratio "i" for either hTISIS or the conventional sample introduction system, and Q_l was the liquid flow rate (see Table 1). As Fig. 2 shows, the hTISIS provided higher signals than the conventional sample introduction system for the four matrices evaluated. The improvement in the analytical signal induced by the hTISIS with respect to the conventional system ranged from 3 (toluene) to nearly 20 times (Premisolv®) compared to the results obtained with the conventional sample introduction system operated at a liquid flow rate around 3 times higher than the hTISIS.

The analysis of pyrolysis oils is complex due to non-spectral interferences. Sample nature could impact every process occurring from the solution nebulization to the signal acquisition.[47] To evaluate matrix effects, four different solutions, containing 25 μg kg^{-1} of As, were prepared by using different solvents: xylene, kerosene, toluene and Premisolv®. Then, to evaluate the effect of the temperature on matrix effects, a relative signal was calculated taking the signal obtained for the xylene solution as reference. When the spray chamber temperature was above 300 °C, equivalent signals were obtained for all the samples, as the average relative signal values were 0.99 ± 0.05 (Fig. S3†). For m/z 91 (mass-shift mode), a similar pattern was observed, with a relative signal of 1.01 ± 0.03 at 400 °C (Fig. S4†). Moreover, the thermal state of the plasma was evaluated by monitoring the $^{36}Ar^{+}$ signal. As revealed in Fig. S5,† using hTISIS at 200 °C or 300 °C did not modify the plasma thermal characteristics. Whereas at 400 °C, a slight drop in $^{36}Ar^{+}$ signal was observed, indicating a minor degradation of the plasma thermal conditions. It is important to note that this change did not affect the degree of mitigation of the matrix effects.

To further evaluate the performance characteristics of the hTISIS system in the determination of As in organic matrices,

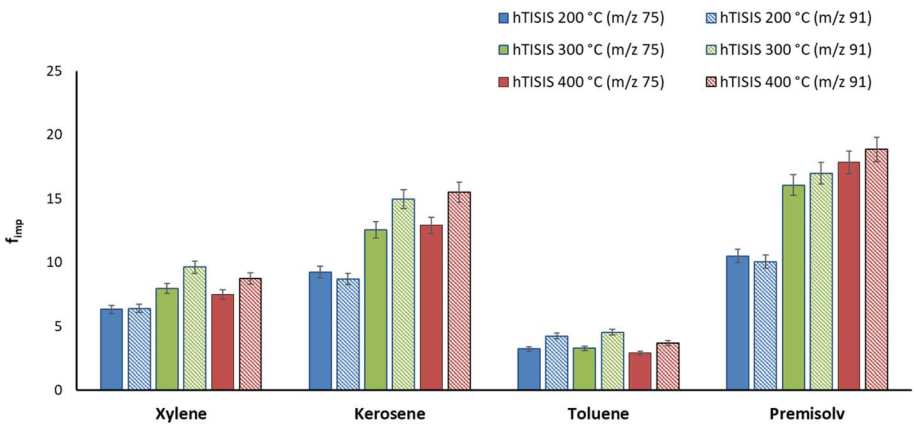

Fig. 2 Improvement factor (f_{imp}) resulting from the use of hTISIS compared to a conventional sample introduction system for the four matrices evaluated and three hTISIS temperatures. $Q_l^{hTISIS} = 30$ μL min^{-1}; $Q_l^{Conventional} = 100$ μL min^{-1}. ICP-MS/MS operating conditions described in Table 1. Oxygen gas flow rate to the reaction cell: 0.075 mL min^{-1}. As concentration using Conostan: 25 μg kg^{-1}.

Table 2 Detection limits and procedural limits of quantification (ng kg^{-1}) for the conventional sample introduction system and the hTISIS at 400 °C. ICP-MS/MS operating conditions described in Table 1. $Q_l^{hTISIS} = 30$ μL min^{-1}; $Q_l^{Conventional} = 100$ μL min^{-1}

	LOD				pLOQ			
	$m/z = 75$ ($^{75}As^+$)		$m/z = 91$ ($^{75}As^{16}O^+$)		$m/z = 75$ ($^{75}As^+$)		$m/z = 91$ ($^{75}As^{16}O^+$)	
Sample	hTISIS (400 °C)	Conventional	hTISIS (400 °C)	Conventional	hTISIS (400 °C)	Conventional	hTISIS (400 °C)	Conventional
Xylene	2	20	0.9	2	60	680	30	60
Kerosene	2	3	0.9	4	60	110	30	130
Toluene	3	3	1.0	3	100	90	30	110
Premisolv®	2	15	1.1	26	50	500	40	850

the detection limits were calculated, according to the following mathematical equation:

$$\mathrm{LOD} = \frac{3s_b}{\mathrm{Sensitivity}} \times \frac{Q_l^{\mathrm{hTISIS}}}{Q_l^{\mathrm{Conventional}}} \quad (2)$$

Except for kerosene, the LODs achieved with hTISIS were either equivalent to or lower than those observed with the conventional sample introduction system (Table 2). The improvement factor varied from 2 to 10. Furthermore, as shown in Table 2, LOD values for $^{75}As^+$ were higher than those obtained by monitoring $^{75}As^{16}O^+$ ions. This observation is particularly notable given that the sensitivity for $m/z = 91$ was markedly lower compared to $m/z = 75$ (Fig. 1). Nevertheless, a significant reduction in blank levels was observed, thus providing extremely low s_b values in the case of $^{75}As^{16}O^+$ ion. Moreover, the procedural limit of quantification (pLOQ) was calculated by taking into account the limit of quantification and the dilution factor. As shown in Table 2, in all cases it was below 1 μg kg^{-1}, with lower values observed for hTISIS operating at 400 °C. These low pLOQs are particularly relevant considering the wide range of arsenic concentrations previously reported in TPO samples. In some samples, the reported As concentration was below 30 μg kg^{-1},[53] highlighting the need for highly sensitive analytical methods.

3.3. Effect of the arsenic chemical form on the sensitivity

One critical aspect in the determination of As using ICP-MS/MS was the influence of the element chemical form on the signal, which is especially pronounced at low liquid flow rates.[25,35–37] This effect was studied for arsenic compounds with different boiling points: trimethylarsine (TMA, b.p. 51 °C), triethylarsine (TEA, b.p. 140 °C), and triphenylarsine (TPA, b.p. 373 °C). Additionally, a commercial Conostan® standard, generally used in organic matrices for ICP calibration, was chosen as a reference compound. For the conventional sample introduction system, the signal order was TPA < TEA < TMA, which perfectly aligned with the order of the boiling point of the compounds. Therefore, once the aerosol was generated, arsenic evaporated more easily if present as TMA, thus delivering a greater mass of this element to the plasma and consequently yielding a higher analytical signal. The relative signal calculated taking the As Conostan solution as reference sample, for TMA was 3.6 (Fig. 3).

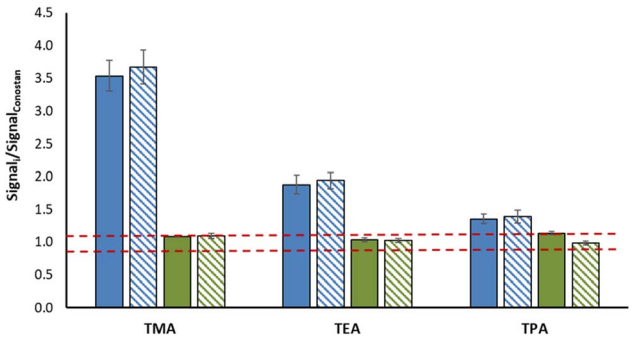

Fig. 3 Relative signal found (mean value ± standard deviation) for $^{75}As^+$ and $^{75}As^{+16}O^+$ for different arsenic solutions, present under different chemical forms, using the conventional sample introduction system and the hTISIS at 400 °C. Sample introduction system: Conventional (blue bars) and hTISIS at 400 °C (green bars). Solid-filled bars: m/z 75; and hatched bars: m/z 91.

In fact, the signal measured for the As Conostan commercial standard was lower than that of the other species.

As demonstrated in previous studies, the use of internal standards was ineffective in correcting the impact of the chemical form on sensitivity.[54] It is important to highlight that the use of Y as internal standard was not sufficient to eliminate the influence of the chemical form of As on sensitivity. Therefore, it is essential to apply an analytical method that could fully mitigate this effect. When hTISIS at 400 °C was used, equivalent signals were achieved for all the As solutions evaluated (Fig. 3). These results were in agreement with those previously shown for other elements such as silicon or chlorine.[45,48,49] Experiments carried at m/z 91 verified the trend shown at m/z 75 (Fig. 3). Furthermore, these observations were validated by analyzing a set of seven TPO samples (A to G in Table S1†), using the hTISIS at 400 °C. Two different sets of calibration standards were tested: one prepared using a Conostan standard solution, and the second set prepared from TPA. Concentrations obtained from both calibration curves were compared, and statistically equivalent concentration values were found (Fig. 4).

3.4. Accuracy evaluation

Accuracy of the hTISIS working at 400 °C coupled to an ICP-MS/MS for arsenic determination in the samples of interest was evaluated by analyzing a fuel oil certified material (NIST 1634c).

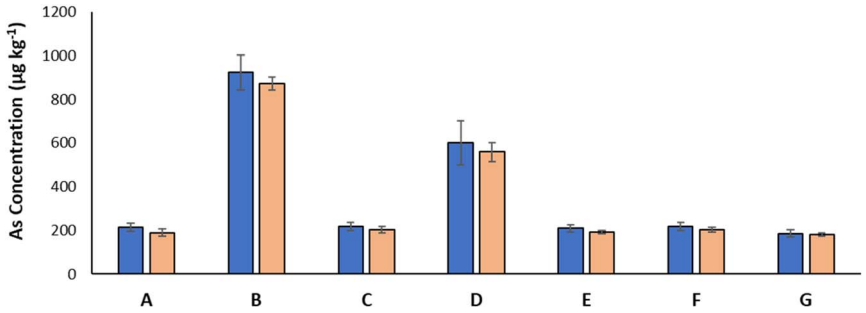

Fig. 4 Arsenic concentration (µg kg^{-1}) for seven pyrolysis oil samples analyzed using the hTISIS at 400 °C. Calibration curve was prepared by using Conostan (blue bars) or TPA (orange bars).

Table 3 As concentrations (µg kg^{-1}; expressed as mean ± t × s/√n; $n = 5$) obtained from the NIST 1634c reference material

	$^{75}As^{+}$		$^{75}As^{16}O^{+}$	
	hTISIS 400 °C	Conventional	hTISIS 400 °C	Conventional
External calibration	137 ± 6	286 ± 23	138 ± 7	274 ± 28
Standard addition	141 ± 7	331 ± 27	140 ± 8	301 ± 23
Certified value	143 ± 6			

Furthermore, to check the accuracy of the method, results obtained by external calibration were compared with those reported by using a standard addition methodology. Table 3 shows the concentrations found by applying the different calibration strategies and the certified value for the analysed sample. To evaluate the results, the difference (Δ_m) between the certified and measured values was compared to the combined uncertainty (U_Δ) of both values (eqn (3)–(5)):

$$\Delta_m = |c_m - c_{CRM}| \quad (3)$$

$$u_\Delta = \sqrt{{s_m}^2 + {u_{CRM}}^2} \quad (4)$$

$$U_\Delta = k \times u_\Delta \quad (5)$$

where c_m is the mean measured value, c_{CRM} is the certified value, s_m is the standard deviation of the measurement, and u_{CRM} is the uncertainty of the certified value.

The expanded uncertainty U_Δ was calculated by multiplying u_Δ by a coverage factor (k), which is usually 2 and represents a confidence level of approximately 95%.[55] Since Δ_m was lower than U_Δ, it was concluded that there were no statistically significant differences between the concentrations obtained by using hTISIS at 400 °C as a sample introduction system and the certified ones (Table S2†). The hTISIS provided identical results irrespectively of the calibration strategy applied (Table 3). However, differences were observed when using the conventional sample introduction system. In fact, even when employing standard addition as a calibration strategy, these differences could not be corrected (Table 3).

Moreover, the accuracy of hTISIS at 400 °C for arsenic determination in TPO samples was further evaluated using three randomly selected samples. Samples were spiked with the Conostan arsenic solution and then analyzed according to an external calibration method having a concentration

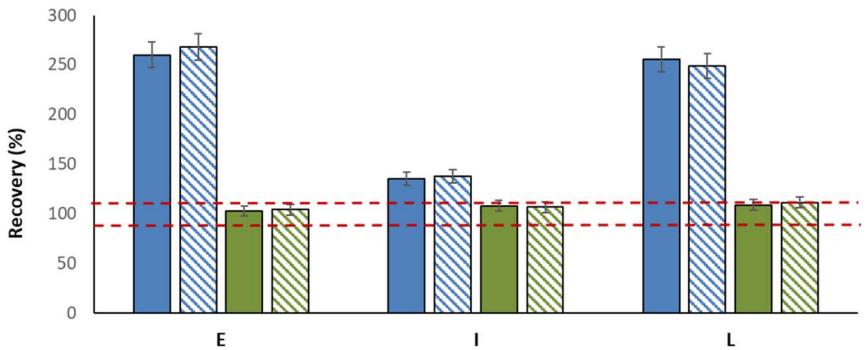

Fig. 5 Recoveries for a set of three TPO samples. Sample introduction system: Conventional (blue bars) and hTISIS at 400 °C (green bars). Solid-filled bars: m/z 75 (on mass in MS/MS mode); and, hatched bars: m/z 91 (mass-shift in MS/MS mode).

corresponding to the spiked one. Fig. 5 plots the recovery results for the m/z 75 and 91 for both sample introduction systems. It was found that the conventional sample introduction system provided recoveries significantly higher than 100%. The matrix effect and especially the As chemical form effect on the signal could be assigned to the differences on the sensitivity with respect to the standards used for external calibration. Meanwhile, the hTISIS, working at 400 °C, afforded recoveries very close to 100%.

3.5. Analysis of real samples

A total of thirteen TPO samples were analyzed. The samples were diluted 10-fold with xylene, and external calibration was applied. An additional experiment was carried out to further evaluate the reliability of the dilution and hTISIS analysis method. The obtained concentrations were compared against those provided by a microwave (MW) digestion method. The diluted digests were analyzed by means of ICP-MS using a conventional sample introduction system. It could be observed that similar data were provided by the two studied analytical methodologies. To evaluate statistical differences, a *t*-Student test was applied to compare the mean values, along with an *F*-test to assess differences in variances ($\alpha = 0.05$, $n_1 = 5$ for the hTISIS, $n_2 = 3$ for the MW method).[46] As shown in Tables 4, S3 and S4,† the results were not significantly different for most of the samples. Statistically significant differences between the two methods were observed in only 2 out of the 13 evaluated cases (samples B and H). The arsenic concentration values obtained ranged from 41 ± 4 to 924 ± 80 μg kg^{-1} (Table 4). Previous studies reported As content below 30 μg kg^{-1}.[53] However, other studies demonstrated the presence of As in these samples at concentrations of 210 μg kg^{-1} and of 590 μg kg^{-1}.[7,56] This wide variability in As content may be related to differences in tire composition due to manufacturing processes, application types (car, truck, other), geographic origin, or long-term use. These factors can influence the accumulation of arsenic-containing compounds in the tire material and, consequently, in the derived pyrolysis oils.

Table 4 Arsenic concentration (μg kg^{-1}; expressed as mean ± t × s/√n; $n_1 = 5$, $n_2 = 3$) for thirteen TPO samples. Statistically significant differences in concentration are highlighted in red

Sample	hTISIS 400 °C	MW digestion
A	213 ± 20	198 ± 32
B	924 ± 80	424 ± 54
C	217 ± 19	190 ± 42
D	600 ± 100	348 ± 48
E	209 ± 17	199 ± 18
F	216 ± 19	190 ± 26
G	185 ± 17	168 ± 29
H	428 ± 48	1380 ± 20
I	84 ± 8	149 ± 55
J	91 ± 11	116 ± 10
K	41 ± 4	55 ± 10
L	98 ± 10	145 ± 40
M	253 ± 32	180 ± 53

4. Conclusions

The determination of arsenic in tire pyrolysis oils is of critical importance due to its strong deactivating effect on hydrotreatment catalysts employed in the upgrading of these complex matrices. Accurate quantification of As at trace levels is essential for the implementation of effective mitigation strategies, such as the design and application of appropriate trapping systems, in order to preserve catalyst activity and ensure the efficiency of downstream processes. In this context, the method developed in the present work represents a significant advancement, offering a robust, sensitive, and practical approach suitable for routine analysis.

The feasibility of accurately determining arsenic concentrations in complex matrices such as tire pyrolysis oils has been clearly demonstrated. The analytical strategy is based on a simple 1 : 10 dilution of the sample in xylene, followed by its analysis using a high-temperature sample introduction system (hTISIS) operating at 400 °C, coupled to an ICP-MS/MS instrument.

The use of hTISIS significantly enhanced analytical performance, providing up to an order of magnitude improvement in sensitivity and lower detection limits compared to conventional sample introduction systems. A procedural limit of quantification (pLOQ) of 0.06 μg kg^{-1} was achieved for xylene-diluted samples, compared to 0.68 μg kg^{-1} using a conventional system.

Furthermore, the hTISIS–ICP-MS/MS configuration enabled the elimination of both non-spectroscopic interferences (matrix effects) and the effect of the arsenic chemical form, achieved through the use of high-temperature conditions (400 °C), and spectroscopic interferences, through the use of oxygen as a reaction gas. As a result, external calibration could be applied using a single set of standards, with both the standards and the samples diluted 1 : 10 in an appropriate solvent such as xylene for the analysis of tire pyrolysis oil samples.

By enabling accurate and reproducible quantification of arsenic across the full range of concentrations reported in real TPO samples, this method provides a valuable analytical tool to support the characterization, valorization, and safe industrial application of pyrolysis oils.

Data availability

The data supporting the findings of this study are available within the article and the ESI.†

Conflicts of interest

There are no conflicts to declare.

Acknowledgements

The authors wish to thank the Spanish Ministry of Science, Innovation, and Universities for the financial support (Project ref. PID2021-127566NB-I00).

References

1 F. Campuzano, J. D. Martínez, A. F. Agudelo Santamaría, S. M. Sarathy and W. L. Roberts, Pursuing the end-of-life tire circularity: An outlook toward the production of secondary raw materials from tire pyrolysis oil, *Energy Fuels*, 2023, **37**, 8836–8866, DOI: 10.1021/acs.energyfuels.3c00847.

2 D. Czarna-Juszkiewicz, P. Kunecki, J. Cader and M. Wdowin, Review in waste tire management—Potential applications in mitigating environmental pollution, *Materials*, 2023, **16**, 5771, DOI: 10.3390/ma16175771.

3 R. Palos, T. Kekäläinen, F. Duodu, A. Gutiérrez, J. M. Arandes, J. Jänis and P. Castaño, Detailed nature of tire pyrolysis oil blended with light cycle oil and its hydroprocessed products using a NiW/HY catalyst, *Waste Manage.*, 2021, **128**, 36–44, DOI: 10.1016/j.wasman.2021.04.041.

4 M. Badlaoui, B. Celse, W. Pejpichestakul, N. Y. P. Cao, M. T. Nguyen, N. Charon, B. Guichard and J. W. Thybaut, Performance Comparison of Tire Pyrolysis Oils in Hydrotreating Toward High-Quality Fuel, *SSRN*, 2024, preprint, DOI: 10.2139/ssrn.5038533, accepted in *Chemical Engineering Journal*.

5 F. Campuzano, A. G. A. Jameel, W. Zhang, A. H. Emwas, A. F. Agudelo, J. D. Martínez and S. M. Sarathy, On the distillation of waste tire pyrolysis oil: A structural characterization of the derived fractions, *Fuel*, 2021, **290**, 120041, DOI: 10.1016/j.fuel.2020.120041.

6 D. Czajczyńska, K. Czajka, R. Krzyżyńska and H. Jouhara, Waste tyre pyrolysis – Impact of the process and its products on the environment, *Therm. Sci. Eng. Prog.*, 2020, **20**, 100690, DOI: 10.1016/j.tsep.2020.100690.

7 S. Somsri, *Upgrading of Pyrolysis Oil, Master Degree Report*, Enviro Systems, Sweden, 2018.

8 M. Banar, V. Akyıldız, A. Ozkan, Z. Cokaygil and O. Onay, Characterization of pyrolytic oil obtained from pyrolysis of TDF (Tire Derived Fuel), *Energy Convers. Manage.*, 2012, **62**, 22–30, DOI: 10.1016/j.enconman.2012.03.019.

9 W. Han, D. Han and H. Chen, Pyrolysis of waste tires: A review, *Polymers*, 2023, **15**, 1604, DOI: 10.3390/polym15071604.

10 S. Martínez, R. Sánchez, J. Lefevre and J. L. Todolí, Multi-elemental analysis of oil renewable fuel feedstock, *Spectrochim. Acta, Part B*, 2022, **189**, 106356, DOI: 10.1016/j.sab.2021.106356.

11 R. Sánchez, J. L. Todolí, C. P. Lienemann and J. M. Mermet, Determination of trace elements in petroleum products by inductively coupled plasma techniques: A critical review, *Spectrochim. Acta, Part B*, 2013, **88**, 104–126, DOI: 10.1016/j.sab.2013.06.005.

12 D. G. Mazumder, Chronic arsenic toxicity & human health, *Indian J. Med. Res.*, 2008, **128**, 436–447.

13 A. Mere, M. Enrico, H. Zhou, E. Tessier and B. Bouyssiere, Arsenic analysis in the petroleum industry: A Review, *ACS Omega*, 2022, **7**, 38150–38157, DOI: 10.1021/acsomega.2c03708.

14 E. Becker, R. T. Rampazzo, M. B. Dessuy, M. G. R. Vale, M. M. da Silva, B. Welz and D. A. Katskov, Direct determination of arsenic in petroleum derivatives by Graphite Furnace Atomic Absorption Spectrometry: A comparison between filter and platform atomizers, *Spectrochim. Acta, Part B*, 2011, **66**, 345–351, DOI: 10.1016/j.sab.2011.04.003.

15 M. V. Reboucas, S. L. C. Ferreira and B. D. B. Neto, Arsenic determination in naphtha by Electrothermal Atomic Absorption Spectrometry after preconcentration using multiple injections, *J. Anal. At. Spectrom.*, 2003, **18**, 1267–1273, DOI: 10.1039/B306101A.

16 M. V. Reboucas, S. L. C. Ferreira and B. D. B. Neto, Behaviour of chemical modifiers in the determination of arsenic by Electrothermal Atomic Absorption Spectrometry in petroleum products, *Talanta*, 2005, **67**, 195–204, DOI: 10.1016/j.talanta.2005.02.01.

17 R. Q. Aucelio and A. J. Curtius, Evaluation of Electrothermal Atomic Absorption Spectrometry for traced determination of Sb, As and Se in gasoline and kerosene using microemulsion sample introduction and two approaches for chemical modification, *J. Anal. At. Spectrom.*, 2002, **17**, 242–247, DOI: 10.1039/B108928P.

18 R. J. Cassella, B. A. R. S. Barbosa, R. E. Santelli and A. T. Rangel, Direct determination of arsenic and antimony in naphtha by Electrothermal Atomic Absorption Spectrometry with microemulsion sample introduction and iridium permanent modifier, *Anal. Bioanal. Chem.*, 2004, **379**, 66–71, DOI: 10.1007/s00216-004-2500-x.

19 Environmental Protection Agency (USA), *Acid digestion of oils for metals analysis by atomic absorption or inductively coupled plasma (ICP) spectrometry, EPA SW-846 Test Method 3031*, 1996.

20 S. Xiu, A. Shahbazi, V. B. Shirley and L. Wang, Swine manure/Crude glycerol co-liquefaction: Physical properties and chemical analysis of bio-oil product, *Bioresour. Technol.*, 2011, **102**, 1928–1932, DOI: 10.1016/j.biortech.2010.08.026.

21 J. Y. Kim, T. S. Kim, I. Y. Eom, S. M. Kang, T. S. Cho, I. G. Choi and J. W. Choi, Characterization of pyrolytic products obtained from fast pyrolysis of chromated copper arsenate (CCA) and alkaline copper quaternary compounds (ACQ) treated wood biomasses, *J. Hazard. Mater.*, 2012, **227–228**, 445–452, DOI: 10.1016/j.jhazmat.2012.05.052.

22 F. Chainet, A. Desprez, S. Carbonneaux, L. Ayouni, M. L. Milliand and C. P. Lienemann, Investigation of the potential of the ICP-MS/MS for total and speciation analysis in petroleum fractions, *Fuel Process. Technol.*, 2019, **188**, 60–69, DOI: 10.1016/j.fuproc.2019.01.013.

23 R. Sánchez, C. Sánchez, C. P. Lienemann and J. L. Todolí, Metal and metalloid determination in biodiesel and bioethanol, *J. Anal. At. Spectrom.*, 2015, **30**, 64–101, DOI: 10.1039/C4JA00202D.

24 S. D. Olsen, S. Westerlund and R. G. Visser, Analysis of metals in condensates and naphtha by Inductively Coupled

Plasma Mass Spectrometry, *Analyst*, 1997, **122**, 1229–1234, DOI: 10.1039/A704017B.

25 F. I. de Albuquerque, C. B. Duyck, T. C. O. Fonseca and T. D. Saint'Pierre, Determination of As and Se in crude oil diluted in xylene by Inductively Coupled Plasma Mass Spectrometry using a dynamic reaction cell for interference correction on 80Se, *Spectrochim. Acta, Part B*, 2012, **71–72**, 112–116, DOI: 10.1016/j.sab.2012.05.008.

26 B. Bouyssiere, F. Baco, L. Savary, H. Garraud, D. L. Gallup and R. Lobinski, Investigation of Speciation of arsenic in gas condensates by capillary gas chromatography with ICP-MS detection, *J. Anal. At. Spectrom.*, 2001, **16**, 1329–1332, DOI: 10.1039/B105765K.

27 S. J. Kumar and S. Gangadharan, Determination of trace elements in naphtha by Inductively Coupled Plasma Mass Spectrometry using water-in-oil emulsions, *J. Anal. At. Spectrom.*, 1999, **14**, 967–971, DOI: 10.1039/A900894B.

28 S. Arnold, A. Rodriguez-Uribe, M. Misra and A. K. Mohanty, Slow pyrolysis of bio-oil and studies on chemical and physical properties of the resulting new bio-carbon, *J. Cleaner Prod.*, 2018, **172**, 2748–2758, DOI: 10.1016/j.jclepro.2017.11.137.

29 J. He, V. Strezov, X. Zhou, R. Kumar and T. Kan, Pyrolysis of heavy metal contaminated biomass pre-treated with ferric salts: Product characterization and heavy metal deportment, *Bioresour. Technol.*, 2020, **313**, 123641, DOI: 10.1016/j.biortech.2020.123641.

30 J. He, V. Strezov, T. Kan, H. Weldekidan, S. Asumadu-Sarkodie and R. Kumar, Effect of temperature on heavy metal(loid) deportment during pyrolysis of avicennia marina biomass obtained from phytoremediation, *Bioresour. Technol.*, 2019, **278**, 214–222, DOI: 10.1016/j.biortech.2019.01.101.

31 Z. Zhang, D. J. Macquarrie, M. De Bruyn, V. L. Budarin, A. J. Hunt, M. J. Gronnow, J. Fan, P. S. Shuttleworth, J. H. Clark and A. S. Matharu, Low-temperature microwave-assisted pyrolysis of waste office paper and the application of bio-oil as an al adhesive, *Green Chem.*, 2015, **17**, 260–270, DOI: 10.1039/C4GC00768A.

32 H. L. Chiang, K. H. Lin, N. Lai and Z. X. Shieh, Element and PAH constituents in the residues and liquid oil from biosludge pyrolysis in an electrical thermal furnace, *Sci. Total Environ.*, 2014, **481**, 533–541, DOI: 10.1016/j.scitotenv.2014.02.083.

33 G. Caumette, C. P. Lienemann, I. Merdrignac, H. Paucot, B. Bouyssiere and R. Lobinski, Sensitivity improvement in ICP MS analysis of fuels and light petroleum matrices using a microflow nebulizer and heated spray chamber sample introduction, *Talanta*, 2009, **80**, 1039–1043, DOI: 10.1016/j.talanta.2009.08.017.

34 A. Leclercq, A. Nonell, J. L. Todolí-Torró, C. Bresson, L. Vio, T. Vercouter and F. Chartier, Introduction of organic/hydro-organic matrices in inductively coupled plasma optical emission spectrometry and mass spectrometry: A tutorial review. Part II. Practical considerations, *Anal. Chim. Acta*, 2015, **885**, 57–91, DOI: 10.1016/j.aca.2015.04.039.

35 C. Pécheyran, C. R. Quetel, F. B. Martin Lecuyer and O. F. X. Donard, Simultaneous Determination of Volatile Metal (Pb, Hg, Sn, In, Ga) and Nonmetal Species (Se, P, As) in Different Atmospheres by Cryofocusing and Detection by ICPMS, *Anal. Chem.*, 1998, **70**(13), 2639–2645, DOI: 10.1021/ac9709615.

36 M. Grotti, F. Ardini, A. Terol, E. Magi and J. L. Todolí, Influence of chemical species on the determination of arsenic using inductively coupled plasma mass spectrometry at a low liquid flow rate, *J. Anal. At. Spectrom.*, 2013, **28**, 1718–1724, DOI: 10.1039/C3JA50159K.

37 E. H. Larsen and S. Stürup, Carbon-enhanced inductively coupled plasma mass spectrometric detection of arsenic and selenium and its application to arsenic speciation, *J. Anal. At. Spectrom.*, 1994, **9**, 1099–1105, DOI: 10.1039/JA9940901099.

38 L. Balcaen, E. Bolea-Fernandez, M. Resano and F. Vanhaecke, Inductively coupled plasma - Tandem mass spectrometry (ICP-MS/MS): A powerful and universal tool for the interference-free determination of (ultra)trace elements - A tutorial review, *Anal. Chim. Acta*, 2015, **894**, 7–19, DOI: 10.1016/j.aca.2015.08.053.

39 E. Bolea-Fernandez, L. Balcaen, M. Resano and F. Vanhaecke, Overcoming spectral overlap *via* inductively coupled plasma-tandem mass spectrometry (ICP-MS/MS). A tutorial review, *J. Anal. At. Spectrom.*, 2017, **32**, 1660–1679, DOI: 10.1039/C7JA00010C.

40 J. Darrouzès, M. Bueno, G. Lespès, M. Holeman and M. Potin-Gautier, Optimisation of ICPMS collision/reaction cell conditions for the simultaneous removal of argon based interferences of arsenic and selenium in water samples, *Talanta*, 2007, **71**, 2080–2084, DOI: 10.1016/j.talanta.2006.09.019.

41 S. D'Illio, N. Violante, C. Majorani and F. Petrucci, Dynamic reaction cell ICP-MS for determination of total As, Cr, Se and V in complex matrices: Still a challenge? A review, *Anal. Chim. Acta*, 2011, **698**, 6–13, DOI: 10.1016/j.aca.2011.04.052.

42 F. C. Pinheiro, C. B. D. Amaral, D. Schiavo and J. A. Nóbrega, Determination of arsenic in fruit juices using Inductively Coupled Plasma Tandem Mass Spectrometry (ICP-MS/MS), *Food Anal. Meth.*, 2017, **10**, 992–998, DOI: 10.1007/s12161-016-0663-7.

43 R. Sánchez, J. L. Todolí, C. P. Lienemann and J. M. Mermet, Universal calibration for metal determination in fuels and biofuels by inductively coupled plasma atomic emission spectrometry based on segmented flow injection and a 350 °C heated chamber, *J. Anal. At. Spectrom.*, 2012, **27**, 937–945, DOI: 10.1039/C2JA10336B.

44 F. Ardini, M. Grotti, R. Sánchez and J. L. Todolí, Improving the analytical performances of ICP-AES by using a high-temperature single-pass spray chamber and segmented-injections micro-sample introduction for the analysis of environmental samples, *J. Anal. At. Spectrom.*, 2012, **27**, 1400–1404, DOI: 10.1039/C2JA30152K.

45 S. Martínez, R. Sánchez, J. Lefevre and J. L. Todolí, Multielemental analyzis of vegetable oils and fats by

means of ICP-OES following a dilution and shot methodology, *J. Anal. At. Spectrom.*, 2020, **35**, 1897–1909, DOI: **10.1039/D0JA00112K**.

46 S. Martínez, R. Sánchez and J. L. Todolí, Inductively coupled plasma tandem mass spectrometry (ICP-MS/MS) for the analysis of fuels, biofuels and their feedstock using a high temperature total consumption sample introduction system operated under continuous sample aspiration mode, *J. Anal. At. Spectrom.*, 2022, **37**, 1032–1043, DOI: **10.1039/D2JA00024E**.

47 R. Sánchez, J. L. Todolí, C. P. Lienemann and J. M. Mermet, Air-segmented, 5-μL flow injection associated with a 200 °C heated chamber to minimize plasma loading limitations and difference of behaviour between alkanes, aromatic compounds and petroleum products in inductively coupled plasma atomic emission spectrometry, *J. Anal. At. Spectrom.*, 2010, **25**, 1888–1894, DOI: **10.1039/C0JA00021C**.

48 R. Sánchez, J. L. Todolí, C. P. Lienemann and J. M. Mermet, Minimization of the effect of silicon chemical form in xylene matrices on ICP-AES performance, *J. Anal. At. Spectrom.*, 2009, **24**, 1382–1388, DOI: **10.1039/B906568G**.

49 S. Martínez, L. Morineau, J. Fernandes and F. Chainet, Novel method for chlorine determination in biofuel lipid feedstock by coupling a total sample introduction system (hTISIS) to an inductively coupled plasma tandem mass spectrometry (ICP-MS/MS), *Anal. Chim. Acta*, 2024, **1301**, 342414, DOI: **10.1016/j.aca.2024.342414**.

50 **https://www.scpscience.com/en/products/categories?id=94&name=premisolv-icp-solvent**.

51 Agilent Technologies; *Agilent 8800 Triple Quadrupole ICP-MS: Understanding Oxygen Reaction Mode in ICP-MS/MS*. December 2012.

52 C. D. Pereira, E. E. Garcia, F. V. Silva, A. R. A. Nogueira and J. A. Nóbrega, Behaviour of arsenic and selenium in an ICP-QMS with collision and reaction interface, *J. Anal. At. Spectrom.*, 2010, **25**, 1763–1768, DOI: **10.1039/C003100C**.

53 M. Banar, V. Akyiliz, A. Özkan, Z. Çokaygil and O. Onay, Characterization of pyrolytic oil obtained from pyrolysis of TDF (Tire Derived Fuel), *Energy Convers. Manage.*, 2004, **24**, 463–469, DOI: **10.1016/j.enconman.2012.03.019**.

54 R. Sánchez, J. L. Todolí, C. P. Lienemann and J. M. Mermet, Effect of the silicon chemical form on the emission intensity in inductively coupled plasma atomic emission spectrometry for xylene matrices, *J. Anal. At. Spectrom.*, 2009, **24**, 391–401, DOI: **10.1039/b806594**.

55 T. Linsinger. *Application Note 1 "Comparison of a Measurement Result with the Certified Value"*. European Commission - Joint Research Centre Institute for Reference Materials and Measurements (IRMM), 2010.

56 G. Uguz and A. Ayanoglu, Characterization of waste tire pyrolysis products by GC, ICP-MS, TGA and DSC, BEU, *J. Sci.*, 2021, **10**, 930–942, DOI: **10.17798/bitlisfen.840108**.